

Testing the broad applicability of the PBEint GGA functional and its one-parameter hybrid form

E. Fabiano,¹ Lucian A. Constantin,² and F. Della Sala^{1,2}

¹*National Nanotechnology Laboratory (NNL), Istituto Nanoscienze-CNR, via per Arnesano 16, I-73100 Lecce, Italy*

²*Center for Biomolecular Nanotechnologies @UNILE,*

Istituto Italiano di Tecnologia, Via Barsanti, I-73010 Arnesano, Italy

(Dated: April 2, 2019)

We review the performance of the PBEint GGA functional (Phys. Rev. B 2010, 82, 113104) recently proposed to improve the description of hybrid interfaces, and we introduce its one-parameter hybrid form (hPBEint). We consider different well established benchmarks for energetic and structural properties of molecular and solid-state systems as well as model systems and newly developed benchmark sets for dipole moments and metal-molecule interactions. We find that PBEint and hPBEint (with 16.67% Hartree-Fock exchange) yield the overall best performance, working well for most of the considered properties and systems and showing a balanced behavior for different problems. In particular, due to their well-balanced accuracy, they perform well for the description of hybrid metal-molecule interfaces.

PACS numbers: 71.10.Ca, 71.15.Mb, 71.45.Gm

INTRODUCTION

Density functional theory [1] (DFT) is nowadays one of the most popular computational methods in quantum chemistry and solid-state physics. Despite its success however, DFT still suffers some limitations due the approximations used in the exchange-correlation (XC) functional, which describes all the quantum electron-electron interactions. In fact, the development and optimization of advanced XC functionals is currently a very active field of research [2].

In the years numerous different XC functionals have been developed, ranging from local density approximations [3] (LDA) to the most advanced orbital-dependent XC functionals [4–8] including exact exchange and selected exact-correlation contributions. The largest popularity in practical applications is however own by two classes of functionals: generalized gradient approximations (GGA) and hybrid functionals. The former are in fact, the method of choice for the investigation of large systems (e.g. in biochemistry or solid-state physics) due to their very favorable cost-to-accuracy ratio, while the latter are the workhorse for computational chemistry. Moreover, the GGA functionals attract theoretical interest because they are the building blocks of the more advanced meta-GGA, hybrid, and hyper-GGA functionals.

Due to their simple form GGA functionals cannot fulfill all the exact constraints of the XC energy and cannot be accurate for both atoms and solids [9, 10]. Therefore, some selective criteria must be employed for their construction. Popular approaches are to develop rather specialized functionals by fitting to specific problems and training sets or by requiring the satisfaction of selected exact constraints of the XC energy. As a result, GGA functionals for molecules (PBE [11], APBE [12], revPBE

[13], RPBE [14], BLYP [15, 16], OLYP [16, 17]) or solids (PBEsol [10], ARPA+ [18], AM05 [19], Wu-Cohen [20]) are obtained. On the other hand, hybrid functionals rely strongly on the underlying GGA approximations and share most of their fundamental drawbacks. In addition, they might suffer from a certain degree of empiricism used to construct the partial inclusion of the Hartree-Fock exchange. Thus, hybrid functionals generally improve over the GGA description but cannot provide a really homogeneous level of accuracy for a wide range of applications, showing occasionally important failures for specific problems (e.g. transition-metal chemistry [21] or metal clusters [22]).

Recently, a growing effort was devoted towards the development of GGA functionals that could provide a well balanced description of a large number of properties. In fact, a wise selection of important exact constraints of the XC energy (as e.g. in PBE or APBE) can be used to optimize the performance of GGA functionals in different contexts [23]. Two noteworthy examples are the PBEint [24] and the HTBS [25] functionals. These functionals are not only equally accurate for molecular and solid-state energetic and structural properties, but potentially important for interface physics, surface science and cluster chemistry. Furthermore, they constitute an optimal starting point for the construction of hybrid functionals of broad applicability.

In particular, the PBEint functional has been developed to respect different exact constraints of the XC energy and to connect the slowly-varying density regime, where the second-order gradient expansion (GE2) of the exchange energy is correct, and rapidly-varying density regime, where the PBE behavior is accurate. Thus, it is reasonably accurate for an important set of molecular and solid-solid state properties and, thanks to its well balanced behavior, especially suited for interface [24], metal-

cluster [22] and surface [26] problems. We recall also that the PBEint XC hole density shows exact properties [26], beyond the PBE and PBEsol ones [27], related to the accurate analysis of metallic surfaces [28].

In this paper we propose a short review and a more detailed assessment of the performance of PBEint for different problems in chemistry and physics. In addition, we use the PBEint functional to build a global hybrid functional and investigate the results of this for different amounts of the Hartree-Fock (HF) exchange mixing. We find that a rather small amount of HF mixing (only 16.67%) gives the best results over a broad range of properties. We recall that global PBE and PBEsol hybrids are instead commonly constructed using 25% and 60% of HF mixing [29], respectively. Thus, the PBEint exchange construction is more compatible with the exact exchange, a result that was already proved in the case of jellium surfaces [26].

THEORY AND COMPUTATIONAL DETAILS

The PBEint functional is constructed considering an exchange functional

$$E_x = \int \rho(\mathbf{r}) \epsilon_x^{\text{unif}}(\rho(\mathbf{r})) F_x(s(\mathbf{r})) d\mathbf{r}, \quad (1)$$

with a PBE-like enhancement factor [11]

$$F_x(s) = 1 + \kappa - \frac{\kappa}{1 + \mu s^2 / \kappa}, \quad (2)$$

where ρ is the electron density, $\epsilon_x^{\text{unif}} = -(3/4)(3/\pi)^{1/3} \rho^{1/3}$ is the exchange energy per particle of the uniform electron gas, and $s = |\nabla\rho| / (2(3\pi^2)^{1/3} \rho^{4/3})$ is the reduced gradient for the exchange. In Eq. (2) the value of the parameter κ can be easily fixed to 0.804 by imposing that the Lieb-Oxford bound [30] for the exchange energy holds locally [11] (i.e. for the exchange energy density at each point in space). The value of the μ parameter can be instead fixed by noting that Eq. (1) has, through second-order, the gradient expansion

$$E_x^{(GE2)} = \int \rho(\mathbf{r}) \epsilon_x^{\text{unif}}(\rho(\mathbf{r})) [1 + \mu s^2] d\mathbf{r}, \quad (3)$$

so that μ can be just identified with the second-order coefficient of the exchange gradient expansion. However, no unique value can be fixed for μ with this condition. In fact, in the slowly-varying density limit ($s \rightarrow 0$) $\mu = \mu^{GE2} = 10/81$ [31], while in the rapidly-varying density limit ($s \gg 1$) $\mu = \mu^{\text{PBE}} = 0.2195$ was found to be a good choice. Finally, from the semiclassical-atom theory it was found $\mu = \mu^{MGE2} = 0.26$ [12, 32]. For the PBEint functional we therefore abandon the idea of a constant μ and consider instead an s -dependent μ with the following

ansatz

$$\mu(s) = \mu^{GE2} + (\mu^{\text{PBE}} - \mu^{GE2}) \frac{\alpha s^2}{1 + \alpha s^2}, \quad (4)$$

with $\alpha = 0.197$. Equation (4) assures that the following minimal constraints are satisfied: i) in the slowly-varying density limit $\mu \rightarrow \mu^{GE2}$; ii) in the rapidly-varying density limit $\mu \rightarrow \mu^{\text{PBE}}$; (iii) the fourth-order term ($\propto s^4$) in the exchange gradient expansion vanishes.

Due to Eq. (4) the exchange enhancement factor of PBEint varies smoothly between that of PBEsol (at small s values) and that of PBE (at larger s values), granting a good description of all possible density regimes and of many different systems from molecules to solids. Note however that the PBEint functional (unlike HTBS) is not a simple interpolation between PBE and PBEsol, but provides instead a physically meaningful (although interpolated) value for the μ parameter at different density-regimes. In fact, a similar construction proved to be useful also in the case of noninteracting kinetic energy functionals [33].

For the correlation part, the PBEint functional utilizes again a PBE-like expression [11]

$$E_c = \int \rho(\mathbf{r}) [\epsilon_c^{\text{unif}}(r_s(\mathbf{r}), \zeta(\mathbf{r})) + H(r_s(\mathbf{r}), \zeta(\mathbf{r}), t(\mathbf{r}))] d\mathbf{r}, \quad (5)$$

with

$$H(r_s, \zeta, t) = \gamma \phi^3 \ln \left(1 + \frac{\beta}{\gamma} \frac{t^2 + At^4}{1 + At^2 + A^2 t^4} \right), \quad (6)$$

where $\rho = \rho_\uparrow + \rho_\downarrow$ is the total density, $r_s = [(4\pi/3)\rho]^{1/3}$ is the local Seitz radius, $\zeta = (\rho_\uparrow - \rho_\downarrow)/\rho$ is the relative spin polarization, $\phi = [(1 + \zeta)^{2/3} + (1 - \zeta)^{2/3}]/2$ is a spin scaling factor, ϵ_c^{unif} is the correlation energy per particle of the uniform electron gas, A is a function of ϵ_c^{unif} and ϕ (see Ref. 11), $t = (3\pi)^{1/6} |\nabla\rho| / (4\phi \rho^{7/6})$ is the correlation reduced gradient, and $\gamma = (1 - \ln 2)/\pi^2$ is a parameter fixed by uniform scaling to the high-density limit of the (spin-unpolarized) correlation energy. The parameter β , which is fixed to 0.066725 in the original PBE by the second-order gradient expansion of the correlation energy, is obtained for PBEint by fitting to a jellium surface reference system: $\beta = \beta^{\text{PBEint}} = 0.052$. In fact, the PBEint correlation can reproduce with high accuracy the wave-vector analysis of the correlation surface energies of jellium slabs of different thickness and r_s [26], outperforming other PBE-like GGA functionals. This result is important to prove the ability of PBEint to describe accurately systems where different density regimes coexist. The value of β^{PBEint} is also intermediate between those of PBE and PBEsol assuring an accurate compromise for a large palette of systems ranging from atoms to solids [26].

Hybrid functional

To construct our hybrid functional we follow the adiabatic connection scheme introduced in Ref. 34 where the XC (hybrid) functional is obtained as the result of the coupling-constant integration

$$E_{xc}^{\text{hyb}} = \int_0^1 E_{xc}^{\text{hyb}}(\lambda) d\lambda, \quad (7)$$

and the following ansatz is used for the hybrid-functional coupling-constant decomposition

$$E_{xc}^{\text{hyb}}(\lambda) = E_{xc}^{\text{GGA}}(\lambda) + (E_x^{\text{HF}} - E_x^{\text{GGA}})(1 - \lambda)^{n-1}, \quad (8)$$

with E_x^{HF} being the Hartree-Fock exchange energy, E_x^{GGA} being the exchange energy of a given GGA functional, and $E_{xc}^{\text{GGA}}(\lambda)$ its coupling-constant decomposition. The parameter n controls the balance between the nonlocal Hartree-Fock and the local GGA exchange at different values of the coupling constant and is related to perturbation theory considerations [34].

If in Eq. (8) we use GGA=PBE and $n=4$, after performing the integration (7), the PBE0 [35] functional (also known as PBE1PBE) is obtained. In this work instead we consider GGA=PBEint and we end up with the hPBEint functional

$$E_{xc}^{\text{hPBEint}} = E_{xc}^{\text{PBEint}} + \frac{1}{n}(E_x^{\text{HF}} - E_x^{\text{PBEint}}). \quad (9)$$

In this case we do not fix the value of the parameter n , but we will consider $n = 4, 5$, and 6 in order to assess the optimal value of this parameter on a broad range of situations. In fact, using a value of $n = 4$ can be better to describe molecular systems (as in PBE0), while larger values of the parameter might be more appropriate for transition-metals, clusters and interfaces.

Computational details

We tested the PBEint and hPBEint functionals for a series of molecular and solid state properties including atomization energies, structural properties, non-bonded interactions and reaction energies. The calculations were performed with the PBEint functional as well as with the hPBEint functional with $n=4, 5$, and 6 . Moreover, calculations employing the PBE [11], PBEsol [10], and PBE0 [35] functionals were also carried out for comparison. In all calculations a def2-TZVPP basis set [36, 37] was employed. For transition metals the core electrons were replaced with effective core potentials (ECP) [38–40]. All calculations were performed at the optimized ground-state geometry, except for those on the DM25 and small interfaces test sets (see below).

All calculations on molecular species were performed with a development version of the TURBOMOLE program package [41]. Calculations on bulk solids were performed with the FHI-AIMS program [42, 43] using the

light basis-set and a $18 \times 18 \times 18$ k -point grid. In this case, scalar relativistic effects were accounted for by the zeroth-order relativistic approximation (ZORA) [44].

In more details, in the present work the following tests were considered:

AE6: Atomization energies of SiH_4 , SiO , S_2 , C_3H_4 , $\text{C}_2\text{H}_2\text{O}_2$, and C_4H_8 ; reference data were taken from Ref. 45. Note that the AE6 test set was build to be representative for the results of the large Database/3 [46], including 109 atomization energies.

W4: Atomization energies from the W4-08woMR test set of Ref. [47]. It includes 83 atomization energies of organic molecules selected from the original W4 test set [48] excluding multi-reference cases.

TM10: Atomization energies of CrH , MnH , CoH , V_2 , Sc_2 , TiO , MnO , CuO , CrF , and CuF . Reference data were taken from Ref. 21.

AUnAE: Atomization energies of the Au_2^- , Au_2 , Au_3 , and Au_5 clusters. Reference data, including relativistic and thermal corrections, were taken from Ref. 22.

K9: Barrier heights and reaction energies of three organic reactions. Namely, $\text{OH} + \text{CH}_4 \rightarrow \text{CH}_3 + \text{H}_2\text{O}$, $\text{H} + \text{OH} \rightarrow \text{O} + \text{H}_2$, and $\text{H} + \text{H}_2\text{S} \rightarrow \text{H}_2 + \text{HS}$. Reference data were obtained from Refs. 45, 49.

HB6: Binding energies of the hydrogen-bond interacting systems $(\text{H}_2\text{O})_2$, $(\text{HF})_2$, $(\text{NH}_3)_2$, $\text{NH}_3\text{-H}_2\text{O}$, $(\text{HCONH}_2)_2$, and $(\text{HCOOH})_2$. Reference data were taken from Ref. 50.

DI6: Binding energies of the dipole-dipole interacting systems $\text{CH}_3\text{Cl-HCl}$, $\text{CH}_3\text{SH-HCl}$, $\text{CH}_3\text{SH-NCH}$, $(\text{H}_2\text{S})_2$, $(\text{HCl})_2$, and $\text{H}_2\text{S-HCl}$. Reference data were taken from Ref. 50.

MGBL19: Bond lengths of H_2 , CH_4 , NH_3 , H_2O , HF , C_2H_2 , HCN , H_2CO , OH , CO , N_2 , F_2 , CO_2 , N_2O , and Cl_2 . Reference values were taken from Ref. 51. Note that this set provides a global assessment over bond lengths involving one hydrogen atom and bond lengths not involving hydrogen atoms, which usually behave differently for different functionals [23].

AUnBL: Bond lengths of Au_2^- , Au_2 , Au_3^+ , Au_3^- , Au_4 , Au_6 (capped pentagon, C_{5v} symmetry), SeAu_2 , and $(\text{ClAuPH}_3)_2$. Reference data were taken from Ref. 22.

F38: Harmonic vibrational frequencies of H_2 , CH_4 , NH_3 , H_2O , HF , CO , N_2 , F_2 , C_2H_2 , HCN , H_2CO ,

TABLE I: Mean absolute errors for different tests as obtained from PBE, PBEint, PBEsol, PBE0, and hPBEint calculations with $n=4, 5, 6$. For each line the best result is indicated by bold face, the worst is underlined. All energies are in kcal/mol (except for COH6). All bond lengths are in mÅ. Vibrational frequencies are in cm^{-1} .

Test	PBE	PBEint	PBEsol	PBE0	hPBEint		
					$n = 4$	$n = 5$	$n = 6$
Organic molecules							
AE6	14.5	24.7	<u>34.9</u>	5.4	12.4	14.3	15.7
W4	10.7	15.5	<u>21.5</u>	5.7	6.3	7.5	8.5
OMRE	6.8	8.2	12.0	9.1	<u>12.8</u>	11.7	11.1
DC9	10.6	15.5	<u>17.6</u>	10.2	13.6	13.9	14.2
K9	7.51	9.09	<u>10.59</u>	3.96	4.90	5.62	6.17
MGBL19	9	<u>10</u>	<u>10</u>	6	9	8	7
F38	56.8	65.4	<u>65.9</u>	51.7	53.2	45.3	45.6
Transition metals							
TM10	13.4	15.5	18.3	<u>18.4</u>	16.2	15.3	12.0
AUnAE ^a	0.3	2.2	<u>4.4</u>	3.4	2.5	1.8	1.3
TMRE	3.7	6.9	9.9	<u>11.1</u>	<u>11.1</u>	9.4	8.3
AUnBL	78	31	25	<u>86</u>	58	56	55
Non-bonded interactions							
HB6	0.4	0.5	<u>1.7</u>	0.5	0.7	0.7	0.6
DI6	0.4	0.4	<u>1.0</u>	0.4	0.4	0.4	0.4
Solid-state properties							
LC6	<u>59</u>	32	22	-	-	-	-
COH6 ^b	0.15	0.14	<u>0.21</u>	-	-	-	-

a) atomization energy per atom.

b) eV/atom.

CO₂, N₂O, Cl₂, and OH. Reference data were taken from Ref. 52

OMRE: Reaction energies of organic molecules. It includes CH₂+H₂ → CH₄, F₂+H₂ → 2HF, C₆H₆+3H₂ → C₆H₁₂, CO+3H₂ → CH₄+H₂O, SO₂+3F₂ → SF₆+O₂, and C₄H₆+C₂H₄ → C₆H₁₀. Reference data were taken from Ref. 53

TMRE: Reaction energies of transition-metal complexes. It includes Ni(CO)₃+CO → Ni(CO)₄, Fe(CO)₄+CO → Fe(CO)₅, $\frac{1}{2}$ Cl₂+CoCl₂ → CoCl₃, and 2FeCl₂ → Fe₂Cl₄. Reference data were taken from Ref. 21.

DC9: Nine reaction energies of medium-size molecules, which are usually treated poorly by DFT methods. Reference values were taken from Ref. 47.

LC6 and **COH6:** Lattice constants and cohesive energies of bulk Na (simple metal), Ag, Cu (transition metals), Si, GaAs (semiconductors), and NaCl

(ionic solid). Reference data were taken from Refs. 54, 55. The LC6 and COH6 tests were not performed for hybrid functionals.

DM25: Dipole moments of molecules. The test set considers a broad range of systems and of dipole moments, ranging from 0.11 to 11.56 Debye. In detail, it includes CO, CFCl₃, furan, OCS, BF, CF₂O, phenol, HCOOH, CH₃SH, HNCO, CH₃COOH, CH₃OCHO, HF, H₂O, CH₃Cl, CH₃ONO, pyridine, H₂CO, ClCN, CuH, HCN, CHOCH₂OH, CH₃NO₂, LiCl, and NH₂(CH=CH)₆NO₂ (denoted as N6). Reference data and geometries of BF, H₂O, CuH, H₂CO, LiCl, and N6 are taken from Ref. 56. The remaining reference data and (experimental) geometries are taken from Ref. 57. All structures are available in supporting information [58].

Small interfaces: Interaction energies of twelve small metal-molecule systems, representative of metal-molecule interfaces. The set includes Au₂-SH, Au₂⁺-N₂, Au₂-SHCH₃, Au₃-SH, Au₃⁺-N₂,

TABLE II: Dipole moments (Debye) for different test molecules as computed with different DFT methods. The mean error (ME), mean absolute error (MAE) and mean absolute relative error (MARE) of each method with respect to reference values are reported in the last lines. For each row the best result is highlighted in bold style, the worst one is underlined.

System	PBE	PBEint	PBEsol	PBE0	hPBEint			Ref.
					$n = 4$	$n = 5$	$n = 6$	
CO	0.22	<u>0.24</u>	0.23	0.10	0.11	0.14	0.15	0.11
CFCl ₃	0.35	<u>0.33</u>	0.35	0.42	0.41	0.40	0.39	0.45
furan	0.59	<u>0.58</u>	0.59	0.66	0.65	0.63	0.62	0.66
OCS	0.75	0.74	0.77	<u>0.80</u>	0.79	0.78	0.77	0.71
BF	1.02	<u>1.04</u>	1.03	0.94	0.95	0.97	0.98	0.79
CF ₂ O	1.12	<u>1.13</u>	1.12	1.12	<u>1.13</u>	<u>1.13</u>	<u>1.13</u>	0.95
phenol	1.25	1.26	1.26	1.28	<u>1.29</u>	1.28	1.28	1.22
HCOOH	1.42	1.42	1.42	<u>1.47</u>	<u>1.47</u>	1.46	1.45	1.41
CH ₃ SH	1.58	1.60	1.61	1.62	<u>1.64</u>	1.63	1.62	1.52
HNCO	1.99	1.99	2.01	<u>2.07</u>	<u>2.07</u>	2.06	2.05	1.61
CH ₃ COOH	1.72	1.72	1.73	<u>1.79</u>	<u>1.79</u>	1.77	1.77	1.70
CH ₃ OCHO	1.86	1.86	1.87	<u>1.89</u>	<u>1.89</u>	1.88	1.88	1.77
HF	<u>1.78</u>	1.79	1.80	1.83	1.84	1.83	1.82	1.82
H ₂ O	1.87	1.88	1.89	1.92	<u>1.93</u>	1.92	1.91	1.85
CH ₃ Cl	<u>1.82</u>	1.83	1.84	1.89	1.90	1.89	1.88	1.87
CH ₃ ONO	2.26	2.27	<u>2.30</u>	2.21	2.21	2.23	2.23	2.05
pyridine	2.22	2.23	2.24	<u>2.27</u>	<u>2.27</u>	2.26	2.26	2.19
H ₂ CO	<u>2.23</u>	2.24	2.25	2.42	2.42	2.38	2.36	2.39
CICN	2.96	2.96	2.98	<u>2.99</u>	<u>2.99</u>	<u>2.99</u>	2.98	2.82
CuH	<u>2.31</u>	2.33	2.28	2.85	2.87	2.76	2.69	2.97
HCN	2.93	2.94	2.95	3.03	<u>3.04</u>	3.02	3.01	2.98
CHOCH ₂ OH	<u>2.40</u>	<u>2.40</u>	2.43	2.57	2.57	2.54	2.51	2.73
CH ₃ NO ₂	3.41	3.41	3.43	<u>3.61</u>	<u>3.61</u>	3.57	3.54	3.46
LiCl	6.90	<u>6.89</u>	6.90	7.06	7.06	7.03	7.01	7.23
N6	16.94	16.95	<u>17.03</u>	15.74	15.77	15.98	16.14	11.56
ME	0.20	0.21	0.22	<u>0.23</u>	<u>0.23</u>	<u>0.23</u>	0.22	
MAE	0.35	0.35	<u>0.36</u>	0.27	0.27	0.28	0.29	
MARE	13.5%	<u>14.4%</u>	14.4	8.0%	7.9%	8.9%	9.8%	
Std. Dev.	1.10	1.10	<u>1.11</u>	0.83	0.84	0.88	0.92	

Au₃-SCH₃, Au₄-SH, Au₄⁺-N₂, and Au₄-SHCH₃. The general structure of the molecule-cluster systems was obtained from Refs. 59–61. Each structure was then reoptimized at the TPSS/def2-TZVPP [36, 37, 62] level of theory. This geometry was successively employed in all the calculations. Reference values were obtained from CCSD(T) calculations [63–65] extrapolated to the complete basis set limit [66]. All structures are available in supporting information [58].

Model systems: We consider four sets of model systems for which exact or extremely accurate solutions are available. Namely, we consider: jellium surfaces, jellium clusters, Hooke’s atoms, and the

hydrogen atom with fractional spin. Additional details are provided in the corresponding subsection later on.

All tests are necessarily not exhaustive, because for computational reasons they only include a relatively small number of systems. Therefore, for specific cases they might be not fully representative of the true performance of the functionals. Nevertheless, since each test set was constructed to have good representativity and because the selected tests cover a broad range of properties and systems, we believe that the present assessment offers a fair overview of the performance of the considered functionals.

TABLE III: Interaction energies (eV) of small organic molecules and gold clusters, computed with different DFT methods. The mean error (ME), mean absolute error (MAE) and mean absolute relative error (MARE) of each method with respect to CCSD(T) are reported in the last lines. For each row the result in best agreement with CCSD(T) calculations is highlighted in bold style, the one in worst agreement is underlined.

System	PBE	PBEint	PBEsol	PBE0	hPBEint			CCSD(T)
					$n = 4$	$n = 5$	$n = 6$	
Au ₂ -SH	1.99	2.20	2.35	<u>1.57</u>	1.72	1.81	1.87	1.98
Au ₂ ⁺ -N ₂	0.99	1.13	1.27	<u>0.84</u>	0.95	0.99	1.01	1.30
Au ₂ -SHCH ₃	0.88	1.04	1.17	<u>0.78</u>	0.90	0.92	0.94	1.24
Au ₃ -SH	3.02	3.20	3.33	<u>2.96</u>	3.09	3.11	3.12	3.15
Au ₃ -N ₂	0.77	0.93	<u>1.06</u>	0.67	0.78	0.74	0.77	0.78
Au ₃ -SCH ₃	2.73	2.90	<u>3.03</u>	2.66	2.79	2.81	2.82	2.88
Au ₄ -SH	<u>2.18</u>	2.36	2.49	2.09	2.23	2.25	2.27	2.48
Au ₄ ⁺ -N ₂	0.67	0.80	<u>0.92</u>	0.58	0.68	0.70	0.72	0.74
Au ₄ -SHCH ₃	0.95	1.11	<u>1.24</u>	0.93	1.04	1.06	1.07	1.05
ME	-0.16	0.01	0.14	<u>-0.28</u>	-0.16	-0.13	-0.11	
MAE	0.16	0.12	0.16	<u>0.28</u>	0.16	0.14	0.12	
MARE	10.61%	8.84%	13.08%	<u>18.89%</u>	10.30%	9.16%	7.72%	
Std Dev	0.14	0.14	<u>0.15</u>	<u>0.15</u>	0.14	0.13	0.12	

RESULTS

Quantum chemistry and solid-state benchmarks

In Table I we report the mean absolute errors (MAE) for different tests, as obtained from PBEint and hPBEint calculations with $n = 3, 4, 5$, with the aim of assessing the performance of the functionals for a broad set of problems. To this end, also PBE, PBEsol, and PBE0 results are reported, since these are natural references for the functionals considered here. Full results of all tests are available in supporting information [58].

For atomization energies of organic molecules, it is well known that GGAs are not very accurate (PBEsol largely fails), while the hybrid functionals perform better than the corresponding GGAs and this is more so for those functionals including a larger fraction of Hartree-Fock exchange [29]. Consequently, PBE0, with a MAE of 5 kcal/mol, is the best functional overall and hPBEint with $n = 4$ yields the best performance among the different variants of hPBEint, reaching almost the PBE0 accuracy for the W4 test. Note that even better results can be obtained by considering higher fractions of exact exchange, as shown for example in Ref. 29 where the admixture of PBE GGA and 32% of exact exchange was found to yield the best results for thermochemistry.

Whereas hybrid functionals improve significantly atomization energies, for reaction energies involving organic molecules the use of hybrid functionals is not so systematically beneficial [47, 67, 68]. In fact, inclusion of Hartree-Fock exchange brings some improvements in

some cases, e.g. for the K9 test where PBE0 and hPBEint with $n = 4$ perform best (see also the BH76RC test [29, 47]), but has small effects for other cases, e.g. G2RC, NBPRC and DC9 tests [47, 67]. Furthermore, in most situations improvements are smaller or even absent when large fractions of Hartree-Fock exchange are used; see for example BHLYP vs BLYP and B3LYP for the BH76RC test [29, 47]. In particular, for the DC9 and OMRE benchmarks considered here, we find that PBE0 brings almost no improvement or even a worsening of the results with respect to PBE. Analogously, the best results at the hPBEint level are obtained when $n = 6$ and a relatively small fraction of nonlocal exchange is used.

Different conclusions are found when one considers the energetic properties of transition-metal complexes or clusters (TM10, AUnAE, TMRE). In this case in fact the use of PBE0 corresponds always to a considerable worsening of the results with respect to PBE. A worsening of the performance is also observed in all cases for hPBEint with respect to PBEint when $n = 4$, although not so marked as for PBE0 vs PBE. Improvements with respect to PBEint are instead found for hPBEint with $n = 6$, which becomes the best functional for TM10, but not for the TMRE test. In this last case hPBEint with $n = 6$ is definitely the best hybrid functional in the present investigation, but slightly worse than PBEint and more than twice worse than PBE. Note however that the TMRE test is a particular difficult test in the context of the present work, because it requires a delicate balancing between the description of metal complexes (best described by

PBEint and PBE) and small organic molecules (best described by hybrids with a large fraction of Hartree-Fock exchange).

Concerning structural properties, hybrid functionals provide a modest improvement for organic molecules (MGBL19 and F38), while they worsen the results for gold clusters (AUnBL). Interestingly, the hPBEint functional with $n = 6$ yields the best results among the different variants of hPBEint, outperforms PBE0 for AUnBL and F38, and gives almost the same result as PBE0 for MGBL19. Thus, the combination of PBEint with 1/6 of Hartree-Fock exchange proves to be a very good choice for structural properties of finite systems.

For non-bonded interactions very good results are obtained at the GGA level using the PBE and PBEint functionals, while poorer results (especially for hydrogen bonds) are given by the PBEsol functional. Hybrid functionals cannot improve the performance of PBE and PBEint, yielding the same MAE as the GGAs for the DI6 test and slightly larger errors for the HB6 test. In this latter case, the best results at the hybrid level are obtained by PBE0, taking advantage of the high accuracy of PBE for the hydrogen bonds, and by hPBEint with $n=6$, taking advantage of the small fraction of Hartree-Fock exchange included.

Concerning solid-state properties, PBEsol is the most accurate for lattice constants, while PBEint is intermediated between it and PBE. However, the limited accuracy of PBEsol for atomic energies causes it to perform poorly for cohesive energies (COH6 test). In this case, where a good description of both bulk solids and atoms is required, PBEint shows a remarkably good performance, due to its well balanced description of different density regimes.

Dipole moments

In Tab. II we report the performance of the different functionals for the description of dipole moments of several test molecules. Benchmarking the dipole moments is not as common as energy and structural tests, nevertheless it is very important to verify the accuracy in the description of density [69, 70]. This test allows in fact to probe indirectly the quality of the description, provided by different functionals, of the electron density distribution in molecules, especially in valence and asymptotic regions. This issue is particularly relevant for GGA functionals, because due to the Coulomb self-interaction error, often they yield a poor description of the electron density far from the atomic core. For the same reasons, an improved description is usually obtained by hybrid approaches.

The general trends outlined above are confirmed by inspection of the results of Tab. II. The smallest errors are obtained by the hybrid functionals, which yield

a global MAE of about 0.28 Debye. A MAE larger by 30% is found instead for GGA methods which perform all very similarly and display a global mean absolute error of about 0.35 Debye. In particular, the best results are obtained when the larger fraction of Hartree-Fock exchange (0.25 for PBE0 and hPBEint with $n=4$) is considered, having a MAE of 0.27 Debye and a MARE below 8%. Nevertheless, good results are achieved also by hPBEint with $n=6$, including only a relatively small fraction of Hartree-Fock exchange.

We note however that the results of Tab. II show for all the functionals several important deviations from the trends depicted above. In fact, for some systems (e.g. HNCO, pyridine, ClCN) the best results are achieved at the GGA level, while PBE0 yields the worst agreement with the reference. Thus, none of the functionals considered here can be labeled as fully reliable for the calculation of the dipole moment of an arbitrary molecular system, but the best compromises are provided by the hPBEint functional with $n=6$, which yields the largest number of results with errors ≤ 0.1 Debye, and PBE0 that yields the best overall MAE and MARE and the largest number of results with errors ≤ 0.2 Debye.

Metal-molecule interfaces

In this subsection we investigate the ability of different functionals to describe hybrid metal-molecule interfaces. These systems pose a difficult challenge to any computational method because of the very different theoretical and numerical issues raised by metallic (extended) systems and molecules. The former are in fact mainly characterized by a slowly-varying density regime and can be properly described with local or semilocal approaches. The latter instead display a significant contribution from rapidly-varying density regions and require a proper treatment of nonlocal interactions.

In view of practical applications it would be nice, of course, to perform tests for the interaction of (functionalized) organic molecules with relatively large metallic clusters or extended (eventually semi-infinite) surfaces. However, for these systems no benchmark value to assess the performance of the methods can be obtained. Accurate experimental values are in fact extremely rare, while high level approaches cannot be applied due to their exceedingly high computational cost. Note also that for large metallic systems static and high-order correlation effects start to play a fundamental role, thus accurate results can only be obtained through very sophisticated methods.

For the reasons mentioned above, in this paper we restrict our attention to a set of relatively small metal-molecule systems composed of small organic molecules interacting with gold clusters of 2, 3 and 4 atoms. For such systems quite accurate benchmark results have been

TABLE IV: Mean absolute errors (MAE) in Hartree or mean absolute relative errors (MARE) for different functionals for the proposed model systems. Best results are in bold style; worst results are underlined.

System	PBE	PBEint	PBEsol	PBE0	hPBEint		
					$n = 4$	$n = 5$	$n = 6$
Jellium surf. energy (MARE)	3.15	2.29	2.32	1.88	2.29	2.29	2.29
Jellium spheres (MAE)	0.46	0.46	0.56	<u>0.57</u>	0.23	0.18	0.17
Hooke's atom (MARE)	3.63	3.45	3.41	<u>3.87</u>	3.78	3.71	3.66
Fractional spin H (MAE)	29.59	27.78	27.63	<u>42.31</u>	40.80	38.19	36.46

TABLE V: XC jellium surface energies (erg/cm²) of the global hybrids PBE0 and hPBEint. The fixed-node diffusion Monte Carlo (DMC) calculations [73, 74] are reported for reference. (1hartree/bohr² = 1.557 × 10⁶erg/cm²). PBE, PBEint, and PBEsol results are taken from Table I of Ref. 24.

r_s	PBE	PBEint	PBEsol	PBE0	hPBEint			DMC
					$n = 4$	$n = 5$	$n = 6$	
2	3265	3378	3374	3312	3378	3378	3378	3392 ± 50
3	741	774	774	756	774	774	774	768 ± 10
4	252	267	267	259	267	267	267	261 ± 8
6	52	56	56	55	56	56	56	53 ± ...

obtained with coupled cluster single, doubles with perturbative triple correction (CCSD(T)) calculations and an assessment of DFT methods could be carried out.

Results are reported in Tab. III. At the GGA level, PBE presents a general tendency to underestimate the interaction energies, while a slight overestimation is observed by PBEint. Finally, PBEsol shows a rather strong overestimation of the interaction energies. Overall, PBEint (with a MAE of 0.16 kcal/mol) is slightly better than PBE and PBEsol. In addition, we note that most of the accuracy for PBE comes from the smallest systems (e.g., Au₂-SH) and larger errors are found when the system size increases. For PBEint an opposite behavior is observed. This trend was already observed for gold clusters [22] and led to the conclusion that PBEint provides the most accurate description of medium and large metal clusters. A similar extrapolation can be supposed to apply also in the present case of metal-molecule interfaces, suggesting that superior results can probably be achieved by PBEint for realistic interfaces. This conclusion is also supported by the observation that for interfaces involving large systems slowly-varying density regions will gain a more important role. Thus PBEint (and partially PBEsol) will be favored over PBE.

The addition of a fraction of Hartree-Fock exchange in the functionals has the effect to reduce the computed interaction energies. This results in a worsening of PBE0 with respect to PBE, but an improvement of hPBEint with respect to PBEint. In fact, all the variants of hPBEint show a MARE lower than PBE and PBEint. In particular, the option with $n = 6$ displays the smallest

MAE and MARE of all the functionals considered in this work. We note also that, because of the small fraction of Hartree-Fock exchange that it includes, hPBEint with $n = 6$ may be supposed to be the best compromise for interfaces of interest in practical application, where large metallic systems are involved [71, 72].

Model systems

In this subsection, we show the performance of PBE0 and hPBEint for several important model-systems:

- (i) jellium surfaces, that contain the main physics of simple metal real surfaces;
- (ii) jellium spheres, that are simple models for simple-metal-particles;
- (iii) Hooke's atom, that represents two interacting electrons in an isotropic harmonic potential of frequency ω . At small values of ω , the electrons are strongly correlated, and at large values of ω , they are tightly bounded, two important cases in many condensed matter applications.
- (iv) The hydrogen atom with fractional spin, a model for the static correlation given by degenerate states.

For all these cases, we use non-self-consistent accurate calculations (for jellium surfaces we use numerical LDA orbitals and densities, for jellium spheres we use accurate exact exchange orbitals and densities, for the Hooke's atom we use exact orbitals and densities, and for the spin-dependent hydrogen atom we use exact-exchange orbitals and densities.) For the hybrids, we use exact-exchange instead of the Hartree-Fock one.

The mean absolute (relative) errors of different functionals for the selected model problems are summarized in Tab. IV. A detailed analysis of the results is given in the following.

Jellium surfaces

The PBEint GGA performs remarkably well for the jellium surfaces, giving very accurate exchange and XC surface energies [24, 26]. Because there are no error compensations between the exchange and correlation parts and the PBEint exchange surface energies are extremely close to the exact-exchange ones [26], any PBEint hybrid will yield the same results as the PBEint GGA and thus be very accurate for the jellium surfaces, as we explicitly show in the Table V. This is a very important result for a functional designed for hybrid interfaces, where the surface physics plays a dominant role. We also mention that PBE0 improves considerably over PBE, but still it is not so accurate in the range $2 \leq r_s \leq 3$, where important metals lie (e.g. Al has $r_s = 2.07$, and Cu has $r_s = 2.67$).

We mention that the RGE2 GGA of Ref. [75] gives similar jellium xc and x-only surface energies as PBEint (see Table 3 and Fig. 3 of Ref. [75] for a detailed analysis of jellium surfaces). Both RGE2 and PBEint have the exchange enhancement factor $F_x \rightarrow 1 + \mu s^2 + O(s^6)$ at small s , and thus the requirement of vanishing $O(s^4)$ terms in this expansion seems very important for accurate jellium x-only surface energies at the GGA level. Note that the exchange part of revTPSS meta-GGA [76], which recovers the 4-th order gradient expansion of the exchange energy, is also accurate for jellium surfaces.

Jellium spheres

In Fig. 1, we show the errors in total energies per electron ($E^{exact}/N - E^{approx}/N$) versus the number of electrons N , for jellium spheres of magic numbers ($N=2, 8, 18, 20, 34, 40, 58, 92$, and 106) with bulk parameter $r_s = 4$. (Note that sodium has $r_s = 3.93$.) The reference values E^{exact}/N represent the corrected DMC data (See Eq. (40) and Fig. 5 of Ref. [77]). We note that HF and EXX perform similarly and badly for this problem [78], whereas LDA is remarkably accurate for large clusters [79, 80]. We also recall that self-consistent effects are very small (see Table I of [81]), such that our non-self-consistent results are expected to give an honest and accurate picture of the performance of various functionals for jellium (metal) particles.

We observe that PBE0 does not improve upon PBE, being even worse for $N \leq 34$. On the other hand, hPBEint (with $n=4, 5$ and 6) significantly improve over the original PBEint for $N \leq 20$. However, on average the best performance is given by hPBEint ($n=6$). This is

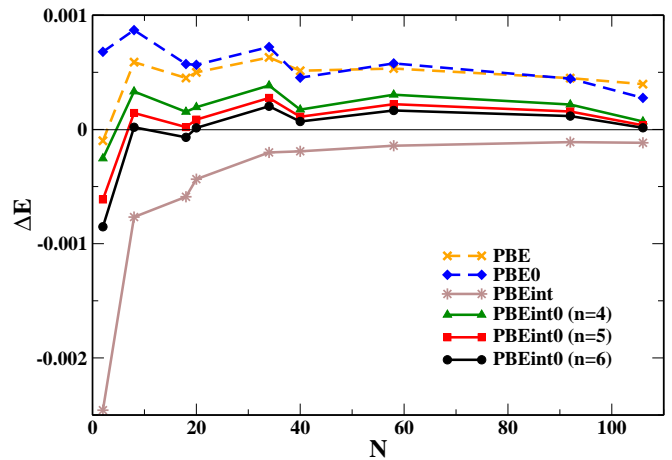


FIG. 1: Errors in total energies per electron ($E^{exact}/N - E^{approx}/N$; Hartree) of jellium spheres for $r_s = 4$. E^{exact}/N represents the corrected DMC data [77]. We use magic neutral clusters with $N=2e^-, 8e^-, 18e^-, 20e^-, 34e^-, 40e^-, 58e^-, 92e^-$, and $106e^-$.

also a very important result for a functional designed for hybrid interfaces, where metal particles play a crucial role.

Hooke's atom

In Fig. 2, we report the relative absolute errors of the hybrids, for the Hooke's atom with several frequencies ω . In the tightly-bounded regime ($r_0 = (\omega^2/2)^{-1/3}$ is small) all the functionals performs similarly, though PBE0 is the best in this extreme case. On the other hand, for $r_0 > 5$, that is the physical case for most of the real applications, the hPBEint hybrids are always better than PBE0, with a superior performance for the $n = 6$ case. However, the errors increase when the strong correlation increases, showing that these global hybrids can not describe satisfactorily the strongly correlated regime.

Hydrogen atom with fractional spin

For the static correlation case, the exact exchange fails badly, and thus the global hybrids usually increase the error in the static correlation with respect to the original GGA. So, from this point of view, the HF mixing should be as small as possible. In Fig. 3, we show that indeed for the different variants of hPBEint increasingly good results are obtained in the series $n=4, 5, 6$. Thus, hPBEint with $n = 6$ has the best performance, while the worst results are obtained with PBE0, which is slightly worse than hPBEint with $n=4$.

We recall however that the N -electron self-interaction error [82], or the delocalization error [83], that is related to the convexity behavior of the functional at fractional

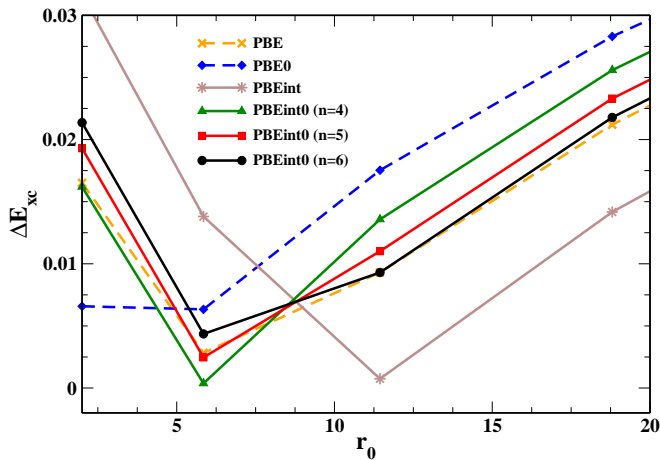


FIG. 2: $\Delta E_{xc} = |(E_{xc}^{app} - E_{xc}^{exact})/E_{xc}^{exact}|$ (Hartree) for the Hooke’s atom with different frequencies. $r_0 = (\omega^2/2)^{-1/3}$ is the classical electron distance [26].

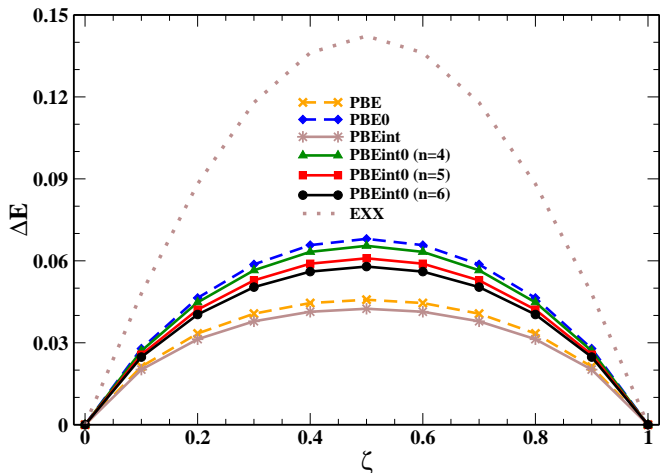


FIG. 3: $\Delta E = E[n, \zeta] - E[n, \zeta = 1]$ (Hartree) versus the spin-polarization ζ .

number of electrons, decreases when the mixing parameter of a global hybrid increases. Thus, the errors of static correlation and of delocalization can not be both reduced by a global hybrid.

Global assessment

To compare the MAE of different tests, we computed, for each group of tests, the MAE relative to PBEint defined as

$$RMAE(\text{method}) \equiv \sum_i \frac{MAE_i(\text{method})}{MAE_i(\text{PBEint})}, \quad (10)$$

where i runs over a given set of tests. The RMAEs for the different classes of tests considered in this work are collected in Tab. VI. To help the analysis of the re-

sults, the benchmarks were divided in two subsets: the *molecular-based* tests including organic molecules, non-bonded interactions, transition metals and dipoles and the *other-systems* including interfaces, solid-state and model systems. For the two groups RMAE-mol and RMAE-other indicate respectively the average RMAE. Finally, RMAE-tot indicates the averaged RMAE among all seven benchmarks.

Among the considered GGAs, PBEint shows a remarkably good performance yielding the best global RMAE-other and RMAE-tot and a RMAE-mol not much higher than PBE and even lower than PBE0. In fact, despite PBEint provides the smallest MAE only in few cases, it has a more balanced performance on different tests. On the contrary, PBE0 and PBE give very accurate results in some cases but behave rather poorly for other tests. The good balance over a broad set of systems and properties is an important feature of the PBEint functional which makes it suitable for applications in complex systems where different situations (or density regimes) may coexist.

Concerning the hybrid functionals similar considerations apply. We observe that functionals incorporating 25% of Hartree-Fock exchange (PBE0 and hPBEint with $n = 4$), despite working very well for energetic properties of organic molecules (see Table I), perform globally worst than their GGA counterparts and other hybrids with a lower Hartree-Fock content, again because of important failures for some properties (e.g., structures and reaction energies). The best overall results are obtained with hPBEint using $n = 6$, which gives also a RMAE-mol of 0.95, (better than PBEint and PBE0). Notably, hPBEint $n = 6$ has in fact a nicely uniform performance for all the tests considered in the present work, being never the worst one and showing a good accuracy for all systems and properties.

Moreover, hPBEint with $n = 6$ and PBEint are the only functionals that can describe rather accurately at the same time energetic and structural properties (this holds also for bulk in the case of PBEint).

CONCLUSIONS

In this paper, we performed an extended study of the PBEint global hybrids. We tested important energetic and structural properties of organic molecules and metal complexes, as well as metal-molecule interfaces. We showed that the hPBEint functional, with the optimal mixing parameter $n=6$, maintains the well-balanced behavior of the PBEint GGA functional, improving the overall accuracy, over a wide range of problems and can thus be successfully employed in complex studies such as the description of hybrid metal-molecule interfaces.

In fact, the PBEint functional and its hybrid forms take benefit from the good treatment of both the slowly-

TABLE VI: Mean absolute errors relative to PBEint (RMAEs; see Eq. (10)) for different sets of tests and all functionals. In the last lines are reported: the global RMAE-mol for molecular properties (organic molecules, non-bonded interactions, transition-metal systems, dipoles); the global RMAE-other for properties not concerning molecular systems (interfaces, solid-state systems, model systems), in this case for hybrid functionals solid-state RMAEs are not considered; the global RMAE-tot for all properties. For each row the best results are highlighted with bold style, the worst ones are underlined

Set	PBE	PBEint	PBEsol	PBE0	hPBEint		
					$n = 4$	$n = 5$	$n = 6$
Organic molecules	0.76	1.00	<u>1.21</u>	0.60	0.79	0.78	0.79
Non-bonded inter.	0.81	1.00	<u>2.84</u>	0.93	1.15	1.11	1.09
Transition metals	1.01	1.00	1.35	<u>1.84</u>	1.41	1.24	1.09
Dipoles	0.99	1.00	<u>1.01</u>	0.76	0.77	0.80	0.82
RMAE-mol	0.85	1.00	<u>1.50</u>	1.03	1.04	0.97	0.93
Interfaces	1.09	1.00	1.19	<u>1.30</u>	1.03	0.98	0.93
Solid-state	<u>1.46</u>	1.00	1.09	-	-	-	-
Model systems	1.12	1.00	1.05	<u>1.18</u>	1.02	0.96	0.93
RMAE-other	1.22	1.00	1.11	<u>1.24</u> ^a	1.03 ^a	0.97 ^a	0.93 ^a
RMAE-tot	1.03	1.00	<u>1.39</u>	1.10 ^a	1.03 ^a	0.98 ^a	0.94 ^a

a) It does not include solid-state.

and rapidly-varying density regimes, granted by Eq. (4). Therefore, despite some limitations for the thermochemistry of organic molecules, they provide reasonably accurate results for all the tests considered and outperform the other functionals for transition metals, hybrid interfaces and solid-state systems. For these reasons the PBEint and hPBEint($n=6$) functional are especially appealing for applications involving transition-metal clusters and/or the interaction of metal clusters with organic molecules. On the other hand, because Eq. (4) is based on a simple GGA ansatz, PBEint-based functionals cannot be expected to outperform specialized functionals for specific problems (e.g. atomization energies of small organic molecules).

In the case of hPBEint the good behavior of the underlying PBEint GGA allows to achieve a good compromise in the overall performance using only a small fraction of Hartree-Fock exchange (16.67% for $n=6$), similarly with the case of hybrid meta-GGAs. This suggests that the PBEint GGA functional could be an interesting starting point for the construction of more advanced hybrids (e.g. local hybrids or screened ones) of good accuracy and large applicability in computational studies.

Finally, we note that a recent work [84] showed that a GGA can be accurate for both solids and molecules, if it satisfies a statistical constraint for atomization energies derived from simple one-electron densities. In particular, the zPBEsol and zPBEint functionals of Ref. [84] significantly improve the atomization energies and other spin-dependent properties, performing the same as the original functionals for any closed-shell system. Thus,

they can be a good starting point for future developments of the hPBEint functional.

ACKNOWLEDGMENTS

We thank TURBOMOLE GmbH for providing us the TURBOMOLE program package and M. Margarito for technical support. This work was funded by the ERC Starting Grant FP7 Project DEDOM, Grant Agreement No. 207441.

-
- [1] Parr, R. G.; Yang, W. Density-Functional Theory of Atoms and Molecules; Oxford University Press; Oxford, 1989.
 - [2] Scuseria, G. E.; Staroverov V. N. Progress in the development of exchange-correlation functionals; in Theory and Applications of Computational Chemistry: The First Forty Years; ed. by Dykstra C., Frenking G., Kim K., Scuseria G. E.; Elsevier, 2005, pp. 669-724.
 - [3] Kohn, W.; Sham, L. J. Phys. Rev. 1965, 140, A1133.
 - [4] Kümmel, S.; Kronik, L. Rev. Mod. Phys. 2008, 80, 3.
 - [5] Della Sala, F. in Chemical Modelling: Applications and Theory, Vol. 7; ed. by M. Springborg; Royal Society of Chemistry, 2010, pp. 115–161.
 - [6] Della Sala, F.; Görling A. J. Chem. Phys. 2001, 115, 5718.
 - [7] Fabiano, E.; Della Sala, F. J. Chem. Phys. 2007, 126, 214102.
 - [8] Bartlett, R. J.; Schweigert, I. V.; Lotrich V. F. J. Mol. Struct.: THEOCHEM 2006, 771, 1-8.

- [9] Perdew, J. P.; Constantin, L. A.; Sagvolden, E.; Burke, K. *Phys. Rev. Lett.* 2006, 97, 223002.
- [10] Perdew, J. P.; Ruzsinszky, A.; Csonka, G. I.; Vydrov, O. A.; Scuseria, G. E.; Constantin, L. A.; Zhou, X.; Burke, K. *Phys. Rev. Lett.* 2008, 100, 136406; (E) *Phys. Rev. Lett.* 2009, 102, 039902.
- [11] Perdew, J. P.; Burke, K.; Ernzerhof, M. *Phys. Rev. Lett.* 1996, 77, 3865.
- [12] Constantin, L. A.; Fabiano, E.; Laricchia, S.; Della Sala, F. *Phys. Rev. Lett.* 2011, 106, 184406.
- [13] Zhang, Y.; Yang, W. *Phys. Rev. Lett.* 1998, 80, 890.
- [14] Hammer, B.; Hansen, L. B.; Nørskov, J. K. *Phys. Rev. B* 1999, 59, 7413.
- [15] Becke, A. D. *Phys. Rev. A* 1988, 38, 3098.
- [16] Lee, C.; Yang, W.; Parr, R. G. *Phys. Rev. B* 1988, 37, 785.
- [17] Handy, N. C.; Cohen, A. J. *Mol. Phys.* 2001, 99, 403.
- [18] Constantin, L. A.; Ruzsinszky, A.; Perdew, J. P. *Phys. Rev. B* 2009, 80, 035125.
- [19] Armiento, R.; Mattsson, A. *Phys. Rev. B* 2005, 72, 085108.
- [20] Wu, Z.; Cohen, R. E. *Phys. Rev. B* 2006, 73, 235116.
- [21] Furche, F.; Perdew, J. P. *J. Chem. Phys.* 2006, 124, 044103.
- [22] Fabiano, E.; Constantin, L. A.; Della Sala, F. *J. Chem. Phys.* 2011, 134, 194112.
- [23] Fabiano, E.; Constantin, L. A.; Della Sala, F. *J. Chem. Theory Comput.* 2011, 7, 3548.
- [24] Fabiano, E.; Constantin, L. A.; Della Sala, F. *Phys. Rev. B* 2010, 82, 113104.
- [25] Haas, P.; Tran, F.; Blaha, P.; Schwartz K. *Phys. Rev. B* 2011, 83, 205117.
- [26] Constantin, L. A.; Chiodo, L.; Fabiano, E.; Bodrenko, I.; Della Sala, F. *Phys. Rev. B* 2011, 84, 045126.
- [27] Constantin, L. A.; Perdew, J. P.; Pitarke, J. M. *Phys. Rev. B* 2009, 79, 075126.
- [28] Pitarke, J. M.; Constantin, L. A.; Perdew, J. P. *Phys. Rev. B* 2006, 74, 045121.
- [29] Csonka, G. I.; Perdew, J. P.; Ruzsinszky, A. *J. Chem. Theory Comput.* 2010, 6, 3688.
- [30] Lieb, E. H.; Oxford, S. *Int. J. Quantum Chem.* 1981, 19, 427.
- [31] Antoniewicz, P. R.; Kleinman, L. *Phys. Rev. B* 1985, 31, 6779.
- [32] Elliott, P.; Burke, K. *Can. J. Chem.* 2009, 87, 1485.
- [33] Laricchia, S.; Fabiano, E.; Constantin, L. A.; Della Sala, F. *J. Chem. Theory Comput.* 2011, 7, 2439.
- [34] Perdew, J. P.; Burke, K.; Ernzerhof, M. *J. Chem. Phys.* 1996, 105, 9982.
- [35] Adamo, C.; Barone, V. *J. Chem. Phys.* 1999, 110, 6158.
- [36] Weigend, F.; Furche, F.; Ahlrichs, R. *J. Chem. Phys.* 2003, 119, 12753.
- [37] Weigend, F.; Ahlrichs, R. *Phys. Chem. Chem. Phys.* 2005, 7, 3297.
- [38] Andrae, D.; Haeussermann, U.; Dolg, M.; Stoll, H.; Preuss, H. *Theor. Chim. Acta* 1990, 77, 123.
- [39] Dolg, M.; Wedig, U.; Stoll, H.; Preuss, H. *J. Chem. Phys.* 1987, 86, 866.
- [40] Fuentealba, P.; Stoll, H.; Szentpaly, L.; Schwerdtfeger, P.; Preuss, H. *J. Phys. B* 1983, 16, L323.
- [41] TURBOMOLE V6.3, 2011, a development of University of Karlsruhe an Forschungszentrum Karlsruhe GmbH, 1989–2007, TURBOMOLE GmbH since 2007; available from <http://www.turbomole.com>.
- [42] Blum, V.; Gehrke, R.; Hanke, F.; Havu, P.; Havu, V.; Ren, X.; Reuter, K.; Scheffler, M. *Comput. Phys. Commun.* 2009, 18, 2175.
- [43] Havu, V.; Blum, V.; Havu, P.; Scheffler, M. *J. Comput. Phys.* 2009, 228, 8367.
- [44] Faas, S.; Snijders, J. G.; van Lenthe, J. H.; van Lenthe, E.; Baerends, E. J. *Chem. Phys. Lett.* 1995, 246, 632.
- [45] Lynch, B. J.; Truhlar, D. G. *J. Phys. Chem. A* 2003, 107, 8996.
- [46] Lynch, B. J.; Truhlar, D. G. *J. Phys. Chem. A* 2003, 107, 3898.
- [47] Goerigk, L.; Grimme, S. *J. Chem. Theory Comput.* 2010, 6, 107.
- [48] Karton, A.; Tarnopolsky, A.; Lamere, J. F.; Schatz, G. C.; Martin, J. M. L. *J. Phys. Chem. A* 2008, 112, 12868.
- [49] Lynch, B. J.; Truhlar, D. G. *J. Phys. Chem. A* 2003, 108, 1460.
- [50] Zhao, Y.; Truhlar, D. G. *J. Chem. Theory Comput.* 2005, 1, 415.
- [51] Zhao, Y.; Truhlar, D. G. *J. Chem. Phys.* 2006, 125, 194101.
- [52] Biczysko, M.; Panek, P.; Scalmani, G.; Bloino, J.; Barone, V. *J. Chem. Theory Comput.* 2010, 6, 2115.
- [53] Grimme, S. *J. Chem. Phys.* 2006, 124, 034108.
- [54] Csonka, G. I.; Perdew, J. P.; Ruzsinszky, A.; Philipsen, P. H. T.; Lebègue, S.; Paier, J.; Vydrov, O. A.; Ángyán, J. G. *Phys. Rev. B* 2009, 79, 155107.
- [55] Haas, P.; Tran, F.; Blaha, P. *Phys. Rev. B* 2009, 79, 085104.
- [56] Zhao, Y.; Schultz, N. E.; Truhlar, D. G. *J. Chem. Theory Comput.* 2006, 2, 364.
- [57] NIST Computational Chemistry Comparison and Benchmark Database. NIST Standard Reference Database Number 101. Release 15b, August 2011, Editor: Russell D. Johnson III. <http://cccbdb.nist.gov/>
- [58] SUPPORTING
- [59] Krüger, D.; Fuchs, H.; Rosseau, R.; Marx, D.; Parrinello M. *J. Chem. Phys.* 2001, 115, 4776.
- [60] Ding, X.; Yang, J.; Hou, J. G.; Zhu, Q. *Journal of Molecular Structure: THEOCHEM* 2005, 755, 9.
- [61] Kuang, X.; Wang, X.; Liu, G. *Applied Surface Science* 2011, 257, 6546.
- [62] Tao, J.; Perdew, J. P.; Staroverov, V. N.; Scuseria, G. E. *Phys. Rev. Lett.* 2003, 91, 146401.
- [63] Purvis III, G. D.; Bartlett, R. J. *J. Chem. Phys.* 1982, 76, 1910.
- [64] Scuseria, G. E.; Janssen, C. L.; Schaefer III, H. F. *J. Chem. Phys.* 1988, 89, 7382.
- [65] Pople, J. A.; Head-Gordon, M.; Raghavachari, K. *J. Chem. Phys.* 1987, 87, 5968.
- [66] Truhlar, D. G. *Chem. Phys. Lett.* 1998, 294, 45.
- [67] Goerigk, L.; Grimme, S. *J. Chem. Theory Comput.* 2011, 7, 291.
- [68] Goerigk, L.; Grimme, S. *Phys. Chem. Chem. Phys.* 2011, 13, 6670.
- [69] Laricchia, S.; Fabiano, E.; Della Sala, F. *J. Chem. Phys.* 2010, 133, 164111.
- [70] Della Sala, F.; Fabiano, E.; Laricchia, S.; D'Agostino, S. Piacenza, M. *Int. J. Quant. Chem.* 2010, 110, 2162.
- [71] Fabiano, E.; Piacenza, M.; D'Agostino, S.; Della Sala, F. *J. Chem. Phys.* 2009, 131, 234101.
- [72] Terentjevs, A.; Steele, M. P.; Blumenfeld, M. L.; Ilyas, N.; Kelly, L. L.; Fabiano, E.; Monti, O. L. A.;

- Della Sala, F. J. Phys. Chem. C 2011, in press; DOI: 10.1021/jp204720a.
- [73] Wood, B.; Hine, N. M. D.; Foulkes, W. M. C.; García-González, P. Phys. Rev. B 2007, 76, 035403.
- [74] Constantin, L. A.; Pitarke, J. M.; Dobson, J. F.; García-Lekue, A.; Perdew, J. P. Phys. Rev. Lett. 2008, 100, 036401 (2008).
- [75] Ruzsinszky, A.; Csonka, G. I.; Scuseria, G. E., J. Chem. Theory Comput. 2009, 5, 763.
- [76] Perdew, J.P.; Ruzsinszky, A.; Csonka, G. I.; Constantin, L. A.; Sun, J., Phys. Rev. Lett. 2009, 103, 026403; *ibid.* 2011, 106, 179902 (E).
- [77] Tao, J.; Perdew, J. P.; Almeida, L. M.; Fiolhais, C.; Kümmel, S. Phys. Rev. B 2008, 77, 245107.
- [78] Sottile F.; Ballone, P. Phys. Rev. B 2001, 64, 045105.
- [79] Constantin L. A.; Ruzsinszky, A. Phys. Rev. B 2009, 79, 115117.
- [80] Lee, D.; Constantin, L. A.; Perdew, J. P.; Burke, K. J. Chem. Phys. 2009, 130, 034107.
- [81] Almeida, L. M.; Perdew, J. P.; Fiolhais, C. Phys. Rev. B 2002, 66, 075115.
- [82] Perdew, J.P.; Parr, R.G.; Levy, M.; Balduz Jr., J.L., Phys. Rev. Lett. 1982, 49, 1691.
- [83] Cohen, A.J.; Mori-Sanchez, P.; Yang, W., Science 2008, 321, 792.
- [84] Constantin, L. A.; Fabiano, E.; Della Sala, F. J., Phys. Rev. B 2011, 84, 233103.